Indian Journal of Chemistry
Vol. 63, May 2024, pp. 473-484
DOI: 10.56042/ijc.v63i5.8969

CyPD inhibition for Alzheimer's: *In silico* screening of phytochemicals from Asian medicinal plants

Smita Jain*[a], Sonali Labhade[b] & Ritesh Bhole[b]

[a] Department of Pharmacy, School of Chemical Sciences and Pharmacy, Central University of Rajasthan, Kishangarh 305 817, Rajasthan, India

[b] Dr. D. Y. Patil Institute of Pharmaceutical Sciences and Research, Pimpri, Pune 411 018, India

E-mail: smitajain1994@gmail.com

Received 21 February 2024; accepted(revised) 16 April 2024

Cyclophilin D (CypD) is a peptidyl-prolyl isomerase F that resides in the mitochondrial matrix and associates with the inner mitochondrial membrane during the mitochondrial membrane permeability transition. CyPD plays a central role in opening the mitochondrial membrane permeability transition pore (mPTP) leading to cell death and has been linked to Alzheimer's disease (AD). Because CypD interacts with amyloid beta (Aβ) to exacerbate mitochondrial and neuronal stress, it is a potential target for drugs to treat AD. Six features' pharmacophores was developed using structure-based drug design for CyPD enzymes and developed pharmacophores were validated using the Gunery-Henry (GH) Scoring method. The GH scores were found in the acceptable range. Further validated pharmacophores were used for exploring the plant-derived database to retrieve the novel hits employing various parameters *viz* fit value, Lipinski rule of five violation, and feature mapping. After the virtual screening process, 11 molecules were retrieved which were further subjected to molecular docking to determine the binding interactions with the CyPD enzyme's active binding sites using the LibDock module in DS 2.0 software. Based on binding energy and binding interactions, three molecules were selected for the *in silico* pharmacokinetics. The knowledge obtained in this study may help to reveal natural compounds that can become potent inhibitors of CyPD.

Keywords: Alzheimer's Disease, Structure-based drug design, Virtual screening, Molecular dynamics simulation, *In silico* pharmacokinetics

Alzheimer's disease (AD) is the prevailing etiology of dementia in the adult population, leading to cognitive and memory impairment because of neuronal stress and subsequent cellular demise[1]. According to contemporary research, it has been shown that malfunction in mitochondria and synapses is an initial pathogenic characteristic of a brain afflicted by AD[2,3]. Previous studies have shown that the buildup of amyloid-β (Aβ) in synaptic mitochondria leads to detrimental effects on both the structure and function of these mitochondria[4,5]. The buildup of Aβ has been shown to have an impact on several cellular processes, including calcium homeostasis, energy metabolism, membrane potential, membrane permeability transition pore (mPTP), mitochondrial dynamics, respiration, and oxidative. It may be feasible to prevent or impede the progression of AD by mitigating the detrimental effects of Aβ-induced mitochondrial toxicity[6,7]. Two potential strategies are the inhibition of Aβ synthesis and the development of Aβ inhibitors. Additional options might potentially include the development of inhibitors that impede the enzymatic activity of secretases, chemicals that disrupt the process of Aβ oligomerization, and the use of "passive vaccines" specifically intended to facilitate the direct clearance of amyloid. As of now, there is a lack of evidence demonstrating significant enhancements in AD symptoms or neuroprotection *via* the utilization of these techniques. Furthermore, the absence of medications during clinical trials might be attributed to apprehensions about potential adverse effects[8–12]. Due to the complex nature of AD and the limited understanding of its molecular biology, it is suggested that the use of multitargeted techniques in the treatment of AD may provide greater efficacy.

Cyclophilin D (CyPD), an enzyme belonging to the peptidyl-prolyl isomerase F family, is localized inside the mitochondrial matrix and forms associations with the inner mitochondrial membrane when the mitochondrial membrane permeability transition occurs. CyPD assumes a pivotal role in the initiation of mPTP opening, ultimately resulting in cellular

demise. The concentration of CyPD was notably increased in neurons located in areas affected by AD. It has been shown that there exists a complex between CypD and Aβ (referred to as CyPD–Aβ) inside the cortical mitochondria of both AD brain and transgenic mice that overexpress a human mutant form of amyloid precursor protein and Aβ (known as Tg mAPP). The use of surface plasmon resonance (SPR) has shown a significant affinity between recombinant CyPD protein and Aβ. The absence of CyPD resulted in a decrease in Aβ-induced mitochondrial and synaptic dysfunction[13]. The specific function of Aβ in mitochondria has not been fully elucidated, however studies have shown that the interaction between mitochondrial Aβ and mitochondrial proteins, such as CyPD, intensifies mitochondrial and brain stress in transgenic mice models of AD[14,15]. The aforementioned results provide evidence that CyPD might be a promising target for therapeutic development in the context of AD. The protective effects of blocking CyPD have been shown to mitigate mitochondrial and synaptic degeneration generated by Aβ and oxidative stress, leading to improvements in both mitochondrial and cognitive function. Currently, the most precise inhibitor of the mPTP is cyclosporin A (CsA). Its mechanism of action involves the inhibition of the peptidyl-prolyl *cis-trans* isomerase (PPIase) activity of CyPD, as shown by previous studies[16–18]. Regrettably, CsA's therapeutic value is limited due to its immunosuppressive mechanism of action, which involves the inhibition of calcineurin, a calcium-dependent protein phosphatase. Additionally, CsA is unable to traverse the blood-brain barrier (BBB). Numerous derivatives of CsA have been consequently synthesized, such as N-Me-Ala-6-cyclosporin A and N-Me-Val-4-cyclosporin. These derivatives exhibit a reduced immunosuppressive impact while retaining their strong inhibitory effects on the PPIase activity of CyPD. As a result, they effectively counteract the opening of mPTP and the initiation of apoptosis[19,20]. In recent studies, Sanglifehrin A (SfA) and antamanide (AA) have been developed with the aim of inhibiting mPTP. However, their potential as therapeutic agents is limited owing to the presence of significant side effects such as neurotoxicity, hepatotoxicity, nephrotoxicity, and low capacity to penetrate the blood-brain barrier (BBB)[21,22]. The effects of the small molecule quinoxaline derivatives synthesized by Guo *et al.* on the calcium-induced mPTP opening need further assessment. Existing inhibitors of CyPD presently exhibit some drawbacks, including limited solubility, inadequate blood-brain barrier penetration, elevated toxicity, and reduced cell permeability. Plants have been documented as a noteworthy natural reservoir of unique chemical compounds that exhibit anti-AD properties, often characterized by little or no adverse effects[23]. Numerous plant extracts and phytochemicals have been documented as having therapeutic potential for AD. These include curcumin, resveratrol, epigallocatechin-3-gallate, morin, delphinidins, quercetin, luteolin, oleocanthal, as well as other phytochemicals like huperzine A, limonoids, and azaphilones. Therefore, the primary objective of this work is to use an *in silico* model to screen chemical compounds derived from Asian medicinal plants in order to identify possible inhibitors of CyPD.

Material and Methodologies

Compounds preparation

The bioactive compounds (1020) with anti-Alzheimer properties that were previously discovered in Asian plants have been gathered from relevant literature. The 2-dimensional structures of these compounds were collected from the PubChem database and visually represented using ChemDraw Professional 15.0.

Structure-based pharmacophore development

X-ray crystallography structure of CyPD (2z6w) was downloaded from the protein databank [24,25]. Structure-based pharmacophore models were developed using the Receptor-Pharmacophore Generation module of Accelrys Discovery Studio 2.0 (26). The approach described herein facilitates the generation of potential pharmacophores by extracting binding characteristics, namely intermolecular non-covalent interactions between receptors and ligands (27). At now, there are six distinct pharmacophore types that are being used, namely: hydrophobic features, aromatic rings, hydrogen bond acceptors (HBA) and donors (HBD), and positive and negative ionizable centers (Pos_ionizable and Neg_ionizable, respectively) [28]. Prior to modeling, it had been verified that both the protein and ligands have entire valence shells. In addition, the methodology included excluded volumes with a radius of 9 Å to indicate the area that is inaccessible to the bound ligand inside the receptor binding site.

Pharmacophore validation and exploration of database

Prior to employing a pharmacophore model in the process of virtual screening, it is essential to conduct a thorough validation. In order to achieve this objective, it is necessary to have a collection of active compounds that have been previously characterized, as well as a collection of inert or decoy compounds that are particular to the target under investigation. A precisely characterized pharmacophore is capable of identifying a greater quantity of active ligands while minimizing the identification of inert or decoy ligands[29]. A literature search was conducted to acquire thirty practically synthesized active inhibitors of CyPD, which were then obtained and visually represented by sketching[30,31].

The decoy compounds used for the purpose of pharmacophore validation were acquired from the DUD-E database. DUD-E is a comprehensive repository including several active and decoy compounds, specifically designed for 102 different targets. Furthermore, it has the capability to produce many decoys for each active ligand[32]. Decoys are intentionally engineered to possess physicochemical features that closely resemble those of active ligands. In the context of DS 2.0, the ligand pharmacophore feature mapping module was used to conduct a screening of active and decoy compounds. The objective was to assess the performance of several pharmacophore models and determine the most effective one. The user has provided a numerical reference without any accompanying text. Additionally, the yield of actives (YA) or recall, the enrichment factor (EF), and the goodness of hit (GH) were determined for each pharmacophore. The most rigorously tested pharmacophore model was used to filter the created database and get the chemicals that best suit the model. The substances that were obtained were assessed for any violations of Lipinski's rule. Moreover, the compounds were subjected to filtration based on their compatibility and estimated values to identify the most efficacious group of molecules as inhibitors of CyPD[32].

Molecular docking

The determination of the optimal conformation of each ligand inside the receptor's binding site, as well as the precise computation of its binding free energy, has significance within the realm of drug development and research. Consequently, the hit compounds that were chosen from the preceding stages were individually subjected to docking simulations inside the active binding region of CyPD employing DS 2.0[33]. The 3-dimensional structure of CyPD protein was downloaded from the protein data bank site (PDB id: 2z6w). DS 2.0 employs LibDock algorithm to identify the binding interactions and calculate binding energy. At first, all retrieved compounds were opened in the 3D window of DS, using CHARMM force field and dreiding minimize tools, most favourable energies were calculated and saved in .sd format. Using the co-crystallized ligand's geometric centroid, the active sites were defined as a sphere of 9Å[34,35]. All retrieved molecules were used for docking onto the active binding sites of the prepared protein. LibDock methods produced more than 100 different poses for each retrieved molecule. During docking, the BEST conformational approach was used, with each molecule having a maximum of 255 conformations within a 20 kcal/mol energy range above the global energy lowest threshold. Ten hotspots were created for each docking. The scoring function along with binding interactions for each conformational posture was used as selection criteria[36] throughout the study. More desired hit molecules were those that showed interactions with required active site residues with a high docking score.

Molecular dynamics simulation (MDs)

The Desmond 2020.1 from Schrödinger, LLC was used to run MD simulations on docked complexes for 2Z6W with Apigenin-7-(6''-malonylglucoside) (A), Javoricin (B) and Muricin-D (C) ligands. The OPLS-2005 force field[37–39] and explicit solvent model with the TIP3P water molecules were used in this system[40] in period boundary salvation box of 10 Å ×10 Å ×10 Å dimensions. Na^+ ions were added to neutralize the charge 0.15 M, NaCl solutions were added to the system to simulate the physiological environment. Initially, the system was equilibrated using an NVT ensemble for 10 ns to retrain over the protein-ligand complexes. Following the previous step, a short run of equilibration and minimization was carried out using an NPT ensemble for 12 ns. The NPT ensemble was set up using the Nose-Hoover chain coupling scheme[41] with the varying temperature, relaxation time of 1.0 ps, and pressure 1 bar maintained in all the simulations. A time step of 2fs was used. The Martyna-Tuckerman–Klein chain coupling scheme[42] barostat method was used for pressure control with a relaxation time of 2 ps. The particle mesh Ewald method[43] was used for calculating long-range electrostatic interactions, and the radius for the coulomb interactions were fixed at 9Å. RESPA

integrator was used for a time step of 2 fs for each trajectory to calculate the bonded forces. Final production run was carried out for 100 ns. The root means square deviation (RMSD), radius of gyration (Rg), root mean square fluctuation (RMSF) and number of hydrogen (H-bonds), and SASA are calculated to monitor the stability of the MD simulations.

Binding free energy analysis

The molecular mechanics combined with generalized Born surface area (MM-GBSA) approach was used to compute the binding free energies of the ligand-protein complexes. The Prime MM-GBSA binding free energy was calculated using the Python script thermal mmgbsa.py in the simulation trajectory for last 50 frames with a 1-step sampling size. The binding free energy of Prime MM-GBSA (kcal/mol) was estimated using the principle of additivity, in which individual energy modules such as coulombic, covalent, hydrogen bond, van der Waals, self-contact, lipophilic, solvation of protein and ligand were collectively added. The equation used to calculate ΔG_{bind} is the following:

$$\Delta G_{bind} = \Delta G_{MM} + \Delta G_{Solv} - \Delta G_{SA}$$

where,

- ΔG_{bind} designates the binding free energy,
- ΔG_{MM} designates difference between the free energies of ligand-protein complexes and the total energies of protein and ligand in isolated form,
- ΔG_{Solv} designates difference in the GSA solvation energies of the ligand-receptor complex and the sum of the solvation energies of the receptor and the ligand in the unbound state,
- ΔG_{SA} designates the difference in the surface area energies for the protein and the ligand.

Drug likeness prediction

A collection of fundamental molecular characteristics, such as molecular weight, the count of hydrogen bond donors and acceptors, and the octanol/water partition coefficient (AlogP), play a crucial role in determining the potential of a molecule to exhibit oral activity in humans. Several computer approaches exist for the prediction of these features. The present work used SwissADME for the computation of these attributes of the identified compounds[44]. The SwissADME website is a valuable online resource that facilitates the calculation of ADME parameters, physicochemical properties, and other descriptors for compounds with drug-like characteristics. The use of Lipinski's rule of five is employed for the purpose of compound filtration. Based on this regulation, a medicine that may be administered orally often adheres to the following criteria: its molecular weight (MW) is equal to or less than 500 Da, the number of hydrogen bond donors (HBDs) is equal to or less than 5, the number of hydrogen bond acceptors (HBAs) is equal to or less than 10, and the octanol/water partition coefficient (A log P) is equal to or less than 5[45]. The aforementioned criteria were computed using SwissADME and then used to filter the hit compounds.

***In silico* pharmacokinetics**

In addition to its effectiveness against the therapeutic target, it is crucial for a drug candidate chemical to possess appropriate ADME qualities, including absorption, distribution, metabolism, and excretion[46]. The estimation of ADME characteristics of compounds has significant relevance in the stages of hit discovery and optimization. Consequently, the ADME attributes of the hits were examined using SwissADME[44]. A further crucial aspect of the drug development process is the anticipation of chemical toxicity. The study used ProTox-II for this purpose[47]. In order to provide a more comprehensive elucidation, it should be noted that ProTox-II is a computer-based laboratory that facilitates the anticipation of many toxicological models, including hepatotoxicity, carcinogenicity, immunotoxicity, mutagenicity, cytotoxicity, stress response pathways, and nuclear receptor signalling pathways.

Results and Discussion

Structure-based virtual screening

The concept of pharmacophore refers to the spatial configuration of crucial steric and electronic characteristics that facilitate the most favourable interaction between a ligand and a macromolecule. The selection of the pharmacophore model may vary depending on the information available, with the choice being either structure-based or ligand-based, corresponding to the availability of target or known ligand data, respectively[48]. The present study involved the construction of a structure-based pharmacophore model. In this work, structure-based pharmacophore model was developed using the X-ray crystal structure

of CyPD (2z6w) which bound cyclosporin A. A pharmacophore model consisting of six characteristics was constructed using DS 2.0 software, as seen in the Fig. 1.

Further validation of developed pharmacophore was done using GH scoring. In this method 780 compounds were used including decoy 750 and total active (Ha) 30 compounds. With CyPD based pharmacophore the following are the initial results; Total hits (Ht) 28, Total active hits (Ha) 24, %Yield of actives 85.71, Enrichment factor (E) 22.28571429, False positives 4 and Goodness of hit score (GH) 0.84, which is greater than the recommended GH scoring value (>0.5), indicating the profoundness of the model (49). The results are shown in Table 1.

The database screening method was conducted utilising the created and verified structure-based pharmacophore in Discovery Studio 2.0. This approach aimed to identify compounds that selectively interact with both the active binding sites of the CyPD free spike protein and the interface between CyPD and the spike protein. The flowchart used in the virtual screening computation conducted in this investigation is shown in Fig. 2. Following the ligand feature mapping process, whereby the ligands were compared with the structure-based pharmacophore, it was seen that out of the total 1000 compounds, 449 compounds were successfully mapped. Furthermore, 16 compounds exhibited complete feature mapping, aligning with all six characteristics of the structure-based pharmacophore, as shown in Table 2.

Molecular docking

The ligand database was constructed using a complete assortment of 16 compounds employed for interaction with the established active site of the CyPD enzyme. A total of 100 conformations of ligand-receptor complexes were created for each molecule, and the conformation exhibiting the highest docking score were selected for further study. Out of the 16 compounds examined, a total of 11 compounds exhibited hydrogen binding interactions with notable docking scores when interacting with the active binding cavities of the CyPD enzyme. This information is presented in Table 3 and visually shown in Fig. 3. Additionally, it was revealed that hydrophobic contacts also had a significant influence. Out of the several docking conformations assessed, compounds A, B, and C had the most favourable docking scores, measuring 94.1, 89.3, and 81.5 kcal/mol, respectively.

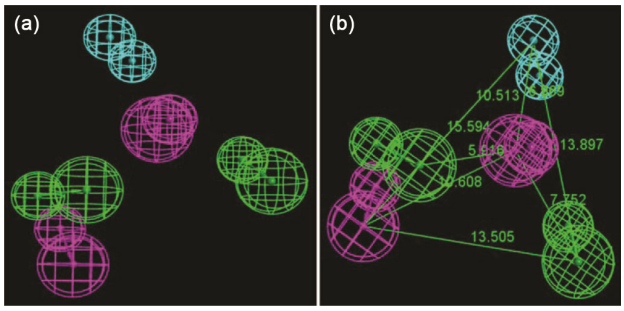

Fig. 1 — (a) Six feature structure-based pharmacophore, (b) interfeature distance among the features

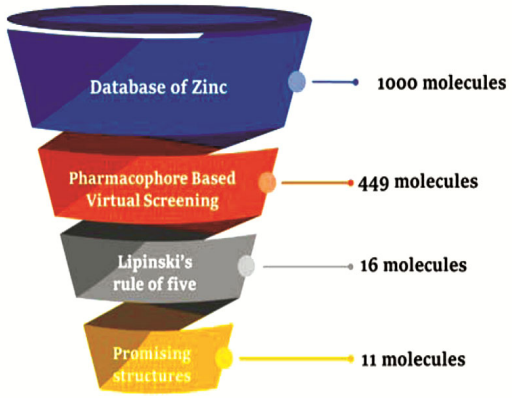

Fig. 2 — Virtual screening of the database

Table 1 — GH scoring

GH Score	CyPD inhibitors
Total molecule (D)	780
Total actives (A)	30
Total hits (Ht)	28
Total active hits (Ha)	24
%Yield of actives[(Ha/Ht) ×100]	85.71429
Enrichment factor (E) [(Ha×D)/(Ht×A)	22.28571
False positives (Ht-Ha)	4
Goodness of hit score	0.842857

Molecular Dynamics Simulation

Molecular dynamics and simulation (MD) studies were carried out to determine the stability and convergence of **2Z6W** with ligands Apigenin-7-(6"-malonylglucoside) (A), Javoricin (B) and Muricin-D (C). Simulation of 100 ns displayed stable conformation while comparing the root mean square deviation (RMSD) values. The RMSD of the Cα-backbone of 2Z6W bound to Apigenin-7-(6’’-malonylglucoside) (A), Javoricin (B), and Muricin-D (C) exhibited an average deviation of 1.7Å, 1.51Å, and 1.66Å (Fig. 4a), respectively.

The trajectories for all complexes seem to reach a plateau after an initial rise, which suggests that each

Table 2 — Feature mapping of selected compounds with structure based developed pharmacophore

Compd	Fit values	Pharmprint	Feature mapping
Annomontacin, *-cis*	3.15986	'100111'	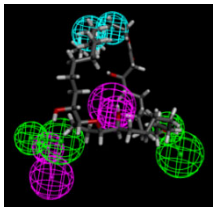
Annonacin-A	1.5747	'111011'	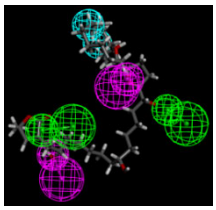
Annonacin, *-cis*	1.23989	'111011'	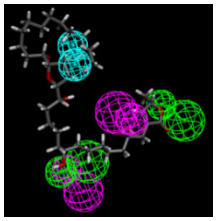
Apigenin_7-(6''-malonylglucoside)	0.285362	'111101'	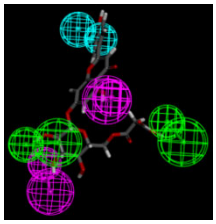
Arctigenin_4'-O-beta-gentiobioside	2.41759	'111011'	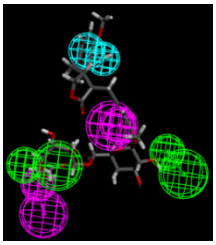
Javoricin	2.1092	'110111'	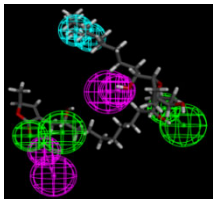
Montanacin-B	1.51114	'101111'	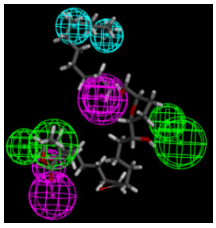

(*contd.*)

Table 2 — Feature mapping of selected compounds with structure based developed pharmacophore (*contd.*)

Compd	Fit values	Pharmprint	Feature mapping
Muricatalin	0.89073	'111111'	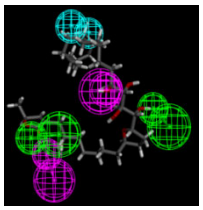
Muricin-A	3.13802	'111011'	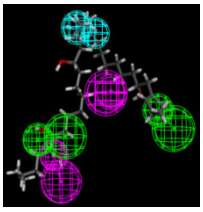
Muricin-D	0.328575	'111111'	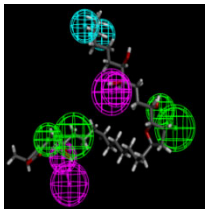
Muricoreacin	0.847196	'111111'	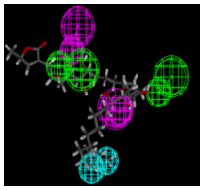
Murihexocin B	2.33468	'101111'	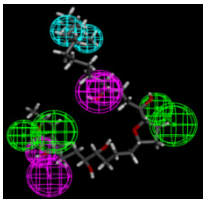
Murihexocin C	0.847196	'111111'	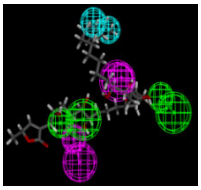
Murisolin	2.28243	'111101'	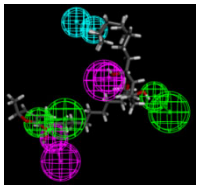
Pectolinarigenin	1.28375	'111101'	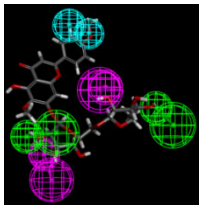

Table 3 — Molecular docking analysis of selected compounds with the CyPD enzyme binding active sites

S. No.	Compound	Docking score (kcal/mol)	Amino acid residues (H-bond distance Å)
1.	Apigenin-7-(6"-malonylglucoside) (A)	94.1	H-His54 (2.34), H-His54 (2.62), H-Phe53 (2.42), O-Thr52 (2.83), O-Ile156 (2.80), O-Thr152 (3.31)
2.	Javoricin (B)	89.3	H-Lys154 (2.53), O-Thr152 (2.70), H-Thr152 (1.98), H-Thr152 (2.58), H-His70 (2.07)
3.	Muricin-D (C)	81.5	H-Asn69 (2.62), O-His70 (3.34), H-Thr52 (2.56), H-Phe53 (2.69), H-Thr152 (2.32), H-Thr152 (2.16)
4.	Arctigenin-4'-O-beta-gentiobioside (D)	79.3	H-Phe53 (2.23), O-Thr152 (2.93)
5.	Montanacin-B (E)	76.4	C-His70 (3.46), O-Thr152 (2.90), O-Thr152 (2.94), H-His54 (2.72)
6.	Annonacin-A (F)	74.2	H-Thr152 (1.89), H-Thr152 (2.37), H-Thr152 (2.28), H-Thr52 (2.42)
7.	Muricin-A (G)	72.9	H-His70 (2.06), H-His70 (2.61), O-Thr52 (3.29), O-His54 (3.50)
8.	Annonacin-cis (H)	71.3	H-His54 (2.42), H-Thr52 (2.36), O-Thr152 (3.15), O-Thr152 (2.89), O-Asn13 (3.08), H-Thr152 (2.27)
9.	Muricapentocin (I)	71.2	H-Lys154 (2.14), H-Thr152 (2.40), H-Thr152 (2.68), O-Thr152 (2.96)
10.	Annomontacin-cis (J)	69.3	H-Thr52 (2.21), O-Thr52 (3.13), O-His54 (3.57), H-His54 (2.16), O-Thr152 (3.14)
11.	Muricatalin (K)	63.1	H-Thr152 (2.18), H-Thr152 (2.05), O-Thr52 (2.87), H-His70 (1.94)

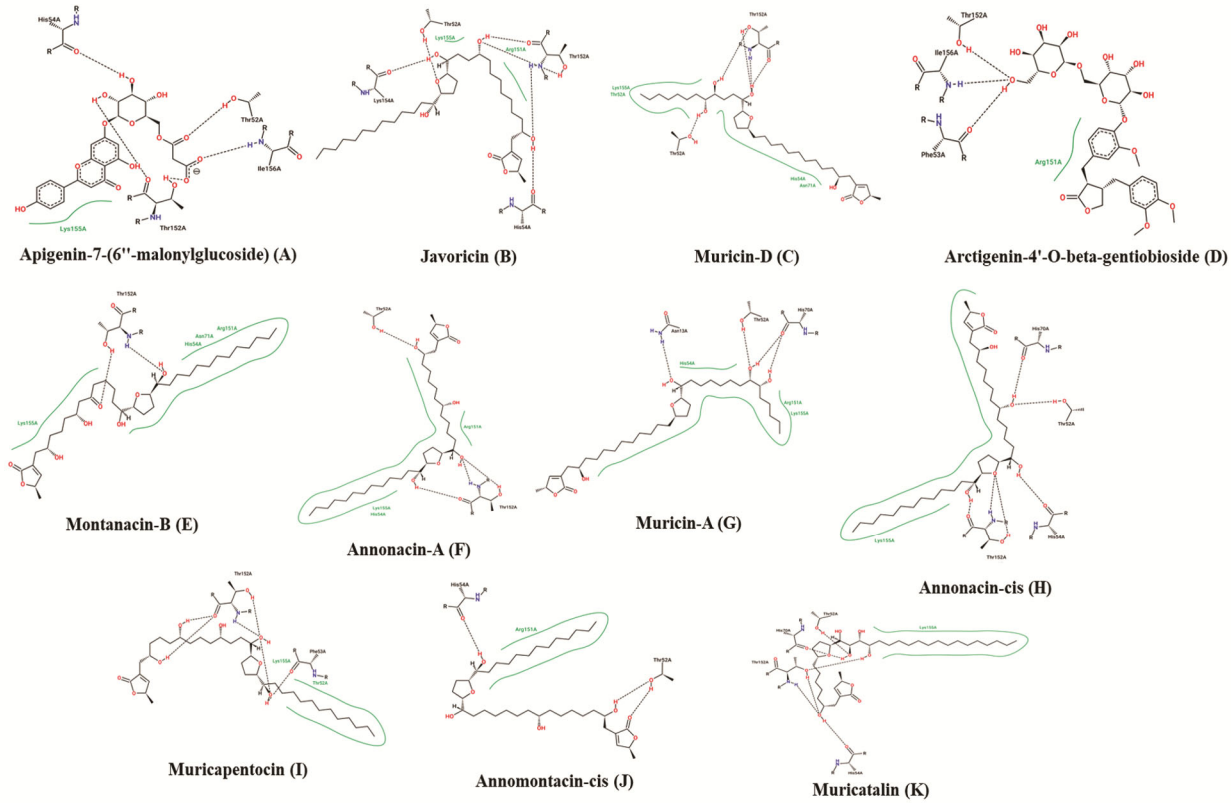

Fig. 3 — Binding interactions of selected compounds with CyPD enzyme active binding sites

system may reach an equilibrium state where the protein's conformational fluctuations are consistent and do not lead to further large-scale structural deviations. A stable RMSD plot during simulation signifies good convergence and stable conformations. Therefore, it can be suggested that all compounds bound to 2Z6W are quite stable in complex due to the higher affinity of the ligand. The graph shows fluctuations in RMSD for all three trajectories, which is common in molecular dynamics simulations due to thermal motion. None of the trajectories show a drastic increase or decrease in RMSD, which might suggest that no large-scale unfolding events are occurring within the timeframe of the simulation. All

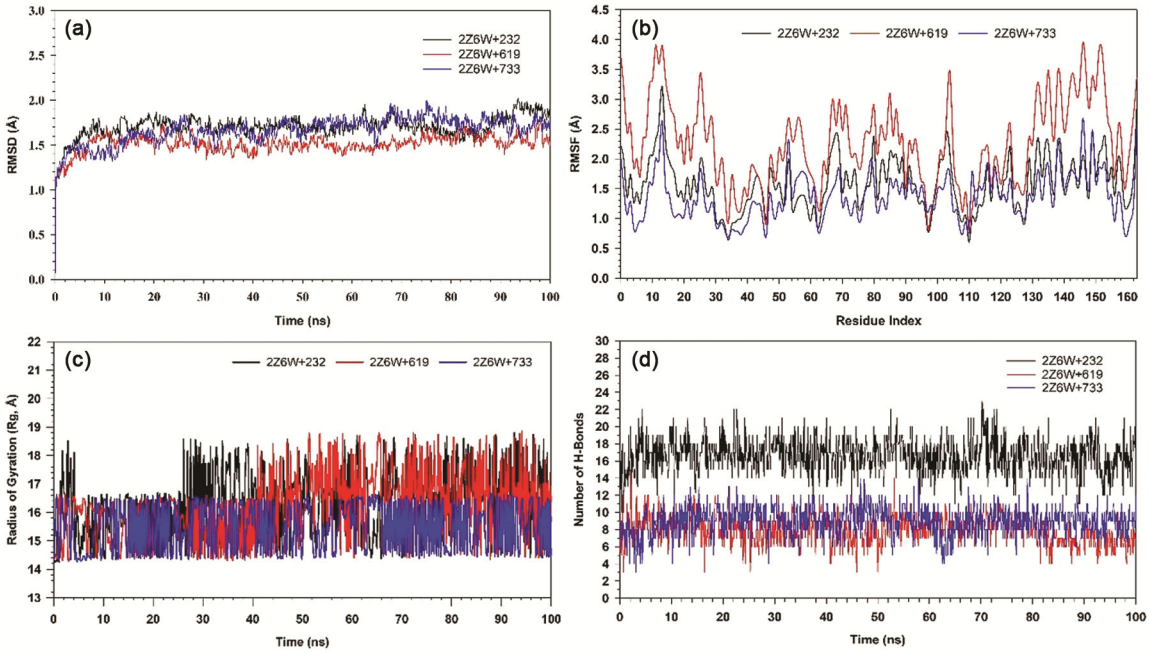

Fig. 4 — MD simulation analysis of 100 ns trajectories of (a) RMSD of Cα backbone of 2Z6W+Apigenin-7-(6''-malonylglucoside) (A) (Black), 2Z6W+Javoricin (B) (Red) & 2Z6W+Muricin-D (C) (Blue) (b) RMSF of Cα backbone of 2Z6W+Apigenin-7-(6''-malonylglucoside) (A) (Black), 2Z6W+Javoricin (B) (Red) & 2Z6W+Muricin-D (C) (Blue), (c) Radius of gyration (Rg) of Cα backbone of 2Z6W+Apigenin-7-(6''-malonylglucoside) (A) (Black), 2Z6W+Javoricin (B) (Red) & 2Z6W+Muricin-D (C) (Blue) (d) Formation of hydrogen bonds in Cα backbone of 2Z6W+Apigenin-7-(6''-malonylglucoside) (A) (Black), 2Z6W+Javoricin (B) (Red) & 2Z6W+Muricin-D (C) (Blue).

three Protein-Ligand complex trajectories remain relatively close together throughout the simulation. This could imply that the differences between ligands Apigenin-7-(6''-malonylglucoside) (A), Javoricin (B), and Muricin-D (C) do not drastically affect the overall stability or structure of the protein. However, there are noticeable differences in the stability of these variants, with the 2Z6W+Apigenin-7-(6''-malonylglucoside) (A) showing a generally lower RMSD, hence potentially more stable, than the 2Z6W+Javoricin (B) and 2Z6W+Muricin-D (C).

Plot 4b root means square fluctuations (RMSF) displayed small spikes of fluctuation in 2Z6W protein and no significant spikes were observed with ligands Apigenin-7-(6''-malonylglucoside) (A) and Muricin-D (C) while compound Javoricin (B) showed particularly high fluctuations around residue numbers 10-15, 50-60, 100-120 and 130-155. This suggests that in these regions, the 2Z6W+Javoricin (B) are particularly dynamic. Most of the residues are less fluctuating during the entire 100 ns simulation (Fig. 4b) indicating the stable amino acid conformations during the simulation time. Therefore, from RMSF plots it can be suggested that the protein structure is rigid during simulation in ligand-bound conformations. It has been found that not a single residue with high fluctuations found in the binding site, indicates all are loop regions. The radius of gyration (Rg) is the measure of compactness of the protein. Here in this study, 2Z6W Cα-backbone bound to ligand Muricin-D (C)displayed the lowest radius of gyration (Rg) (Fig. 4c). This suggests that ligand Muricin-D (C) forms a highly compact orientation with the protein. The complex 2Z6W+Apigenin-7-(6''-malonylglucoside) (A) shows the greatest variation in Rg, with values spiking and dipping more dramatically than the other two simulations. This could indicate that this variant of the protein experiences more significant conformational changes throughout the simulation. 2Z6W+Javoricin (B) and 2Z6W+Muricin-D (C) lines are less variable and remain closer together, suggesting that these variants maintain more consistent compactness over time. While there are fluctuations, none of the lines show a consistent upward or downward trend, which suggests that no large-scale unfolding or compacting events are happening within the observed timeframe. The plots indicate that all three complexes fluctuate in their degree of compactness during the simulation, with 2Z6W+Apigenin-7-(6''-malonylglucoside) (A)

showing the most variation. This variability might be important for the protein's function if it involves conformational changes. The more consistent Rg values for 2Z6W+Javoricin (B) and 2Z6W+Muricin-D (C) indicate that they may be more stable in their compactness, which could reflect on their structural integrity during the simulation. The lack of fluctuations suggests that the protein does not undergo significant folding or unfolding during the 100 ns timescale of the simulation. Several hydrogen bonds between protein and ligand suggest the interaction and stability of the complex. The number of hydrogen bonds showed high numbers with all ligands, throughout the simulation time of 100 ns (Fig. 1b). The average consistent number of hydrogen bonds observed between 2Z6W with Apigenin-7-(6''-malonylglucoside) (A) is 17, with Javoricin (B), 8, and with Muricin-D (C), 9 H-bonds (Fig. 4d).

Molecular Mechanics Generalized Born Surface Area (MM-GBSA) calculations

Utilizing the MD simulation trajectory, the binding free energy along with other contributing energy in the form of MM-GBSA is determined for all three protein-ligand complexes. The results (Table 1) suggested that the maximum contribution to ΔG_{bind} in the stability of the simulated complexes was due to ΔG_{bind}Coulomb, ΔG_{bind}vdW, $\Delta G_{bind}H_{bond}$ and ΔG_{bind}Lipo, while, ΔG_{bind}Covalent and ΔG_{bind}SolvGB contributed to the instability of the corresponding complexes. 2Z6W+Javoricin (B) complex has comparatively lower binding free energies than other complexes (Table 4). These results supported the potential of 2Z6W+Javoricin (B)having a relatively high affinity towards protein and the ability to form stable protein-ligand complexes.

***In silico* pharmacokinetics**

Table 5 shows the pharmacokinetics and toxicological parameters of the investigated compounds, including GI absorption, blood brain barrier permeability, *P*-glycoprotein (pgp) substrate, PAINS, synthetic accessibility, bioavailability score, interaction with principal cytochrome p450 isoenzymes (CYP1A2, CYP2C19, CYP2C9, CYP2D6 and CYP3A4), and toxicities. All of the lead compounds had a low level of gastrointestinal (GI) absorption, suggesting their propensity to be absorbed *via* the human small intestine. In addition, it should be noted that with the exception of Apigenin-7-(6''-malonylglucoside) and Arctigenin-4'-O-beta-gentiobioside, none of the compounds under

Table 4 — Binding free energy components for the 6LU7+Marvinjs-8A calculated by MM-GBSA.

Energies (kcal/mol)	2Z6W+Apigenin-7-(6''-malonylglucoside) (A)	2Z6W+Javoricin (B)	2Z6W+Muricin-D (C)
ΔG_{bind}	–23.46+2.78	–26.54+2.47	–20.38+6.08
ΔG_{bind}Lipo	–1.71+0.19	–6.77+1.62	–7.30+1.98
ΔG_{bind}vdW	–25.97+1.35	–31.81+1.79	–21.95+2.99
ΔG_{bind}Coulomb	–28.45+8.43	–6.33+3.07	–9.47+3.71
$\Delta G_{bind}H_{bond}$	–1.95+0.34	–0.68+0.45	–0.94+0.50
ΔG_{bind}SolvGB	35.16+7.21	16.74+2.94	17.52+3.18
ΔG_{bind}Covalent	3.51+1.08	2.32+1.55	1.76+1.84

Table 5 — ADME characteristics of selected compounds

Molecule	A	B	C	D	E	F	G	H	I	J	K
TPSA	213.42	116.45	116.45	232.52	133.52	116.45	116.45	116.45	136.68	116.45	136.68
iLOGP	0.78	6.83	6.54	2.37	6.31	6.79	7.06	6.68	6.51	7.43	6.38
GI absorption	Low	Low	Low	Low	Low	Low	Low	Low	Low	Low	Low
BBB permeant	No	No	No	No	No	No	No	No	No	No	No
Pgp substrate	Yes	No	No	Yes	No	No	No	No	No	No	No
CYP1A2 inhibitor	No	No	No	No	No	No	No	No	No	No	No
CYP2C19 inhibitor	No	No	No	No	No	No	No	No	No	No	No
CYP2C9 inhibitor	No	No	No	No	No	No	No	No	No	No	No
CYP2D6 inhibitor	No	No	No	No	No	No	No	No	No	No	No
CYP3A4 inhibitor	No	Yes	Yes	No	Yes	Yes	Yes	Yes	Yes	Yes	Yes
log Kp (cm/s)	–8.38	–3.71	–4.3	–10.81	–5.23	–3.96	–3.96	–3.96	–4.88	–3.37	–4.37
Lipinski #violations	3	1	1	3	1	1	1	1	1	1	1
Bioavailability Score	0.11	0.55	0.55	0.17	0.55	0.55	0.55	0.55	0.55	0.55	0.55
PAINS #alerts	0	0	0	0	0	0	0	0	0	0	0

consideration demonstrate substrate activity for *P*-glycoprotein (*P*-gp). The PAINS alert is indicative of the propensity of chemicals to selectively target a particular biological molecule, as opposed to exhibiting non-specific reactivity towards biological targets. Based on the projected parameters, it has been determined that the substances under investigation do not exhibit characteristics of either a substrate or an inhibitor for the major isoenzyme of CYP450. It is noteworthy to observe that all lead compounds exhibit a high degree of synthetic accessibility and possess a favourable Bioavailability score.

The assessment of toxicity included the examination of many factors, including acute oral toxicity, AMES mutagenesis, carcinogenicity, and hepatotoxicity. No evidence of mutagenic or carcinogenic effects was seen in any of the substances that were subjected to testing. Nevertheless, it was anticipated that the chemicals Annonacin-A, Annonacin-cis, Montanacin-B, Muricapentocin, Muricatalin, Muricin-A, and Muricin-D would demonstrate hepatotoxicity.

Conclusion

In this study, the focus was on exploring potential inhibitors of CyPD for the treatment of AD. AD, characterized by cognitive and memory impairment, has been linked to mitochondrial and synaptic dysfunction induced by the accumulation of amyloid-β (Aβ). The enzyme CyPD, found in elevated concentrations in neurons affected by AD, plays a crucial role in initiating mPTP opening, leading to cellular demise.

The research delved into the identification of compounds from Asian medicinal plants that could serve as inhibitors of CyPD. Through a comprehensive computational approach, including structure-based pharmacophore development, molecular docking, drug-likeness prediction, and *in silico* pharmacokinetics, potential inhibitors were screened and evaluated.

The results revealed several compounds, such as Apigenin-7-(6"-malonylglucoside), Javoricin, and Muricin-D, showing promising interactions with the active binding sites of CyPD, as evidenced by significant docking scores and hydrogen binding interactions. These compounds exhibited desirable drug-like properties, including low gastrointestinal absorption, no *P*-glycoprotein substrate activity, and favorable pharmacokinetic profiles.

The findings open avenues for further experimental validation and development of these compounds as potential therapeutic agents for AD. The study's emphasis on utilizing natural compounds from Asian medicinal plants adds to the growing interest in exploring plant-based remedies for complex diseases like AD. However, it is essential to acknowledge the preliminary nature of the findings, and subsequent *in vitro* and *in vivo* studies are warranted to validate the efficacy and safety of these potential inhibitors.

Acknowledgements

The authors would like to acknowledge the Central University of Rajasthan for providing financial support to this investigation.

References

1 Mortby M E, Black S E, Gauthier S, Miller D, Porsteinßon A, Smith E E & Ismail Z, *Int Psychogeriatrics*, 30 (2018) 171.
2 Jara C, Cerpa W, Tapia-Rojas C & Quintanilla R A, *Front Neurosci*, 14 (2021) 1.
3 Jain S, Bisht A, Verma K, Negi S, Paliwal S & Sharma S, *Cell Biochem Funct*, 40 (2022) 106.
4 Du H, Guo L, Fang F, Chen D, A Sosunov A, M McKhann G, Yan Y, Wang C, Zhang H, Molkentin J D, Gunn-Moore F J, Vonsattel J P, Arancio O, Chen J X & Yan S D, *Nat Med*, 14 (2008) 1097.
5 Manczak M, Anekonda TS, Henson E, Park BS, Quinn J & Reddy P H, *Hum Mol Genet*, 15 (2006) 1437.
6 Hauptmann S, Scherping I, Dröse S, Brandt U, Schulz KL, Jendrach M, Leuner K, Eckert A & Müller W E, *Neurobiol Aging*, 30 (2009) 1574.
7 Valasani K R, Hu G, Chaney M O & Yan S S, *Chem Biol Drug Des*, 81 (2013) 238.
8 Stains C I, Mondal K & Ghosh I, *Chem Med Chem*, 2 (2007) 1674.
9 Ghosh A K, Venkateswara R K, Yadav N D, Anderson D D, Gavande N, Huang X, Terzyan S & Tang J, *J Med Chem*, 55 (2012) 9195.
10 Ogura A, Morizane A, Nakajima Y, Miyamoto S & Takahashi J, *Stem Cells Dev*, 22 (2012) 374.
11 Parker M F, Barten D M, Bergstrom C P, Bronson J J, Corsa J A, Dee M F, Gai Y, Guss V L, Higgins M A, Keavy D J, Loo A, Mate R A, Marcin L R, McElhone K E, Polson C T, Roberts S B & Macor J E, *Bioorg Med Chem Lett*, 22 (2012) 6828.
12 Jain S, Singh R, Paliwal S & Sharma S, Mini-Rev Med Chem, 23 (2023) 2097.
13 Du H, Guo L, Zhang W, Rydzewska M & Yan S, *Neurobiol Aging*, 32 (2011) 398.
14 Takuma K, Yao J, Huang J, Xu H, Chen X, Luddy J, Trillat A-C, Stern D M, Arancio O & Yan S S, *FASEB J*, 19 (2005) 1.
15 Ma Z, Zhang J, Du R, Ji E & Chu L, *Biol Pharm Bull*, 34 (2011) 1684.
16 Tanveer A, Virji S, Andreeva L, Totty N F, Hsuan J J, Ward J M & Crompton M, *Eur J Biochem*, 238 (1996) 166.
17 Griffiths E J & Halestrap A P, *Biochem J*, 274 (1991) 611.
18 Galat A & Metcalfe S M, *Prog Biophys Mol Biol*, 63 (1995) 67.

19 Khaspekov L, Friberg H, Halestrap A, Viktorov I & Wieloch T, *Eur J Neurosci*, 11 (1999) 3194.

20 Nicolli A, Basso E, Petronilli V, Wenger RM & Bernardi P, *J Biol Chem*, 271 (1996) 2185.

21 Clarke S J, McStay G P & Halestrap A P, J Biol Chem, 277 (2002)34793.

22 Azzolin L, Antolini N, Calderan A, Ruzza P, Sciacovelli M, Marin O, Mammi S, Bernardi P & Rasola A, *PLoS One*, 6 (2011) e16280.

23 Guo H X, Wang F, Yu K Q, Chen J, Bai D L, Chen K X, Shen X & Jiang H L, *Acta Pharmacol Sin*, 26 (2005) 1201.

24 Cheung J, Rudolph M J, Burshteyn F, Cassidy M S, Gary E N, Love J, Franklin M C & Height J J, *J Med Chem*, 55 (2012) 10282.

25 Košak U, Brus B, Knez D, Šink R, Žakelj S, Trontelj J, Pišlar A, Šlenc J, Gobec M, Živin M, Tratnjek L, Perše M, Sałat K, Podkowa A, Filipek B, Nachon F, Brazzolotto X, Więckowska A, Malawska B, Stojan J, Raščan I M, Kos J, Coquelle N, Colletier J-P & Gobec S, *Sci Rep*, 6 (2016) 39495.

26 Pal S, Kumar V, Kundu B, Bhattacharya D, Preethy N, Reddy M P & Talukdar A, *Comp Struc Biotech J*, 17 (2019) 291.

27 Giordano D, Biancaniello C, Argenio M A & Facchiano A, *Pharmaceuticals*, 15 (2022) 646.

28 Maia E H B, Assis L C, Oliveira T A, Silva A M & Taranto A G, *Front Chem*, 8 (2020) 481382.

29 Vuorinen A & Schuster D, Methods,71 (2015)113.

30 Grosdidier A, Zoete V & Michielin O, *Nucleic Acids Res*, 39 (2011) W270.

31 Grosdidier A, Zoete V & Michielin O, *J Comput Chem*, 32 (2011) 2149.

32 Lu S H, Wu J W, Liu H L, Zhao J H, Liu K T, Chuang C K, Lin H Y, Tsai W B & Ho Y, *J Biomed Sci*, 18 (2011) 1.

33 Zhou S, Yuan Y, Zheng F & Zhan C G, *Chem Biol Interact*, 308 (2019) 372.

34 Zhou Y, Lu X, Yang H, Chen Y, Wang F, Li J, Tang Z, Cheng X, Yang Y, Xu L & Xia Q, *Molecules*, 24 (2019) 4217.

35 Jain S, Sharma S, Paliwal A, Dwivedi J, Paliwal S, Paliwal V, Paliwal S & Sharma J, *Med Chem Res*, 33 (2023) 136.

36 Ojha M, Kumar A, Prasun C, Nair M S, Chaturvedi S, Paliwal S K & Nain S, *J BiomolStruct Dyn*, 41 (2023) 805.

37 Bowers K J, Chow D E, Xu H, Dror R O, Eastwood M P, Gregersen B A, Klepeis J L, Kolossvary I, Moraes M A, Sacerdoti F D, Salmon J K, Shan Y & Shaw D E, *IEEE*, . (2007) (https://ieeexplore.ieee.org/stamp/ stamp.jsp?tp=&arnumber=4090217).

38 Chow E, Rendleman C, Bowers K, Dror R, Gullingsrud J, Sacerdoti F D & Shaw D E, *Desmond Performance on a Cluster of Multicore Processors*, (2008), (https://www.deshawresearch.com/publications/Desmond_Performance_Cluster.pdf).

39 Shivakumar D, Williams J, Wu Y, Damm W, Shelley J &Sherman W, *J Chem Theory Comp,* 6 (2010) 1509.

40 Jorgensen W L, Chandrasekhar J, Madura J D, Impey R W & Klein M L, *J Chem Phys*, 79 (1983) 926.

41 Martyna G J, Tobias D J & Klein M L, *J Chem Phys*, 101 (1994) 4177.

42 Martyna G J, Klein M L & Tuckerman M, *J Chem Phys*, 97 (1992) 2635.

43 Toukmaji A Y & Board J A, *Comp Phys Comm*, 95 (1996) 73.

44 Jukic M, Milosavljević F, Molden E & Ingelman-Sundberg M, *Trends Pharmacol Sci*, 43 (2022) 1055.

45 Sharma R, Yadav D & Yadav R, *Bioint Res Appl Chem*, 12 (2022) 7503.

46 Wang Z, Yang H, Wu Z, Wang T, Li W, Tang Y & Liu G, *Chem Med Chem*, 13 (2018) 2189.

47 Silva V B D, Andrade P D, Kawano D F, Morais P A B, Almeida J R D, Carvalho I, Taft C A & Silva C H T D P, *Fut Med Chem*, 3 (2011) 947.

48 Andrade C, Silva D & Braga R, *Curr Drug Meta*, 15 (2014) 514.

49 Jang C, Yadav D K, Subedi L, Venkatesan R, Venkanna A, Afzal S, Lee E, Yoo J, Ji E, Kim S Y & Kim M-H, *Sci Rep*, 8 (2018) 14921.